Conf-9105188--1

(to Fracture Toughness)

INFLUENCE OF CRACK DEPTH ON REACTOR PRESSURE VESSEL STEEL*

Timothy J. Theiss and John W. Bryson
Engineering Technology Division
Oak Ridge National Laboratory
Oak Ridge, Tennessee

CONF-9105188--1

DE91 012537

To be published as an ASTM STP Special Technical Publication

Presented at the ASTM Symposium on Constraint Effects in Fracture
May 8, 1991
Indianapolis, Indiana

DISCLAIMER

*Research sponsored by the Office of Nuclear Regulatory Research, U.S. Nuclear Regulatory Commission under Interagency Agreement 1886-8011-9B with the U.S. Department of Energy under Contract DE-AC05-84OR21400 with Martin Marietta Energy Systems, Inc.

ASTM Symposium on Constraint Effects in Fracture to be held May 8-9, 1991, in Indianapolis, IN

Authors' Names:
Timothy J. Theiss[1], and John W. Bryson[1]

Title of Paper:
Influence of Crack Depth on the Fracture Toughness of Reactor Pressure Vessel Steel

Authors' Affiliations:
[1]Engineer, Oak Ridge National Laboratory, PO Box 2009, MS-8056, Oak Ridge, TN 37831-8056

ABSTRACT: The Heavy Section Steel Technology Program (HSST) at Oak Ridge National Laboratory (ORNL) is investigating the influence of flaw depth on the fracture toughness of reactor pressure vessel (RPV) steel. Recently, it has been shown that, in notched beam testing, shallow cracks tend to exhibit an elevated toughness as a result of a loss of constraint at the crack tip. The loss of constraint takes place when interaction occurs between the elastic-plastic crack-tip stress field and the specimen surface nearest the crack tip. An increased shallow-crack fracture toughness is of interest to the nuclear industry because probabilistic fracture-mechanics evaluations show that shallow flaws play a dominant role in the probability of vessel failure during postulated pressurized-thermal-shock (PTS) events.

Tests have been performed on beam specimens loaded in 3-point bending using unirradiated reactor pressure vessel material (A533 B). Testing has been conducted using specimens with a constant beam depth (W = 94 mm) and within the lower transition region of the toughness curve for A533 B. Primarily two crack depths have been considered: a = 50 and 9 mm (a/W = 0.5 and 0.1). Three specimen thicknesses (B = 50, 100, and 150 mm) have been used to examine the influence of different out-of-plane constraint conditions on the test results. All tests resulted in cleavage failures. Test results indicate a significantly higher fracture toughness associated with the shallow flaw specimens compared to the fracture toughness determined using deep-crack (a/W = 0.5) specimens. The toughness increase is comparable with the toughness increase found at the University of Kansas using steels whose stress-strain properties bound those of A533 B. Test data also show little influence of thickness on the fracture toughness for the current test temperature (-60 °C). The Irwin β_c correction has been modified to account for shallow flaws and was used to estimate the shallow-flaw toughness based on the results from the deep-crack specimens.

KEY WORDS: elastic-plastic fracture mechanics, constraint, shallow-crack fracture toughness, test data, reactor pressure vessel material, Irwin β_c correction

Nomenclature

a = crack depth
B = specimen thickness
CMOD = crack mouth opening displacement
CTOD = crack tip opening displacement
E = Elastic Modulus
IPTS = Integrated Pressurized-Thermal-Shock
K_{Ic} = Critical Stress Intensity Factor, plane strain fracture toughness
K_c = Non-plane-strain fracture toughness
LLD = load line displacement
m = constraint parameter
RPV = Reactor Pressure Vessel
PWR = Pressurized Water Reactor
PTS = Pressurized-Thermal-Shock
RT_{NDT} = reference nil-ductility transition temperature
SENB= single edge notch bend
T = temperature
W = specimen depth
σ_y = Yield Strength
ν = Poisson's Ratio
β_c = Beta-c

Introduction

Recent investigations into the influence of crack depth on fracture toughness at the University of Kansas have shown a significant increase in toughness of steel specimens containing shallow flaws **[1, 2]**. Similar research is being jointly carried out by the Edison Welding Institute in the U. S. and The Welding Institute in the U. K. The phenomenon of elevated shallow-crack fracture toughness appears to be caused by the relaxation of crack-tip constraint due to the proximity of a free surface. The elevated shallow-crack fracture toughness occurs in the lower transition range where cleavage fracture takes place but at temperatures slightly above the lower shelf. Significant increases (factor of 2.5 to 4.0) in CTOD caused by shallow cracks were found for both A36 and A517 material at the University of Kansas. A36 steel is a low-strength, high-strain-hardening material, while A517 is a high-strength, low-strain-hardening material. The strength and strain hardening properties of A533 B are between those of A36 and A517. It was anticipated therefore that a significant increase in the toughness of shallow-flaws in A533 B would also take place **[3]**.

Current reactor pressure vessel (RPV) life assessments are strongly dependent on the ability of the vessel material to withstand load in the presence of a flaw (i.e. sufficient fracture toughness). An accurate determination of the fracture toughness of an RPV is particularly important for pressurized-thermal-shock (PTS) loading. The fracture toughness used in RPV life assessments is a function of $T\text{-}RT_{NDT}$ and to date has been determined using deep-notch specimens to provide conservative results. Probabilistic fracture mechanics evaluations of operating nuclear facilities in the Integrated Pressurized Thermal Shock (IPTS) studies have shown that shallow, surface flaws rather than deep cracks in the reactor vessel contribute predominantly to the calculated probability of vessel failure **[4-6]**. The dominance of shallow rather than deep flaws in the probabilistic fracture mechanics evaluations is due in part to the higher density of shallow flaws

assumed to exist in the vessel wall, the increased radiation damage near the inside surface, and the severity of the thermal shock on the vessel surface. IPTS studies indicate that roughly 95% of all the flaws that are predicted to initiate during the dominant transients for the three vessel models considered were 25 mm (1 in.) deep or less [4-6]. Moreover, the majority of these initiations took place at temperatures below RT_{NDT}. The temperatures of interest roughly correspond with the lower transition region of the toughness curve for A533 B material. In other words, a large number of the initiation events for an RPV in PTS analyses originate from shallow flaws and occur within the lower transition region where the shallow-flaw increase in the fracture toughness has been shown to take place.

Preliminary estimates of the shallow-crack toughness for A533 were made, based on the results for A36 and A517, and these estimates were used to determine the impact of a shallow flaw elevated toughness in PTS analyses. These analyses revealed that PTS analyses could potentially be significantly impacted by considering the shallow-crack toughness in reactor pressure vessel material [7]. The Heavy Section Steel Technology Program (HSST) is therefore investigating the influence of flaw depth on the fracture toughness of reactor pressure vessel (RPV) steel [3, 8].

The ultimate goal of the shallow-crack investigation is the generation of a limited data base of elastic-plastic fracture toughness values appropriate for shallow flaws in a reactor pressure vessel and the application of these data to reactor vessel life assessments. To meet these objectives, the HSST experimental shallow-crack work is divided into two phases: a development phase and a production phase. Complementary analytical investigations are also in progress. During the experimental development phase the laboratory techniques necessary for shallow-crack testing will be established and verified through several development beam tests. Once the testing capabilities are confirmed, the toughness of shallow-cracks will be compared with the toughness measured using deep-crack specimens as a part of the production phase of the project. The test results reported in this paper are a part of the developmental phase of this project. While, the results to date have been encouraging, they should still be considered preliminary.

Test Specimen

The specimen configuration chosen for testing shallow cracks in the HSST shallow-crack project is the single-edge-notch-bend (SENB) specimen with a through-thickness crack (as opposed to surface crack). The bend specimen better simulates the varying stress field in a reactor wall under PTS conditions. In addition, previous shallow-crack work has utilized SENB specimens [1, 2]. The straight-through notch simulates an infinitely long, two-dimensional, axially-oriented crack in an RPV. To better simulate the conditions of a shallow-flaw in the wall of a reactor vessel, the specimen depth W and thickness B should be as large as practicable. PWR vessel walls are nominally 200 to 280 mm thick (8 to 11 in.). A ≈100-mm-deep (4-in.) beam has been selected for use in the HSST shallow-crack project. The stress state in beams of this size simulate the stress state in a flawed vessel wall. To maintain consistency with ASTM standards, the beams are being tested in three-point bending. All testing is being conducted on reactor material (A533 Grade B, Class 1) [9] with the cracks oriented in the L-S orientation to maintain consistency with the conditions of an RPV.

Pretest Analysis

A preliminary numerical study was conducted to help determine instrumentation requirements, to provide pretest analytical predictions of the global and local beam behavior, and to define the crack depth(s) that would be expected to exhibit an elevated shallow crack toughness. Crack depth to beam depth ratios (a/W) of 0.05, 0.10, 0.15, 0.20, and 0.50 were analyzed. The beam depth was held constant at 100 mm (4 in.); the

span was set at 4W. The ADINA-87 [10] finite element code was used to perform plane strain, elastic-plastic (von Mises, isotropic hardening) analyses of the beams loaded in three-point bending (to the plane strain limit load). A multilinear stress-strain representation of A533 B material tensile properties at T = - 60 °C (-76 °F) was utilized.

Eight-noded isoparametric quadrilateral elements with reduced 2 x 2 integration order were employed throughout the modeling. Special collapsed quadrilaterals, i.e., wedge elements, were used at the crack tip in order to simulate blunting and to provide a 1/r singularity at the crack tip. A total of 412 elements and 1335 nodes were used in the modeling for each of the five crack depths. A "crack tip region" which always had the same mesh structure was obtained by simply translating the block through the depth and renumbering the surrounding nodes and elements, hence, each model had roughly the same finite element discretization.

The results of the numerical study indicated a fundamental difference in the nonlinear stresses surrounding the crack tip. The elevated fracture toughness associated with shallow flaws is due to a loss of constraint which is indicated by the nonlinear stresses surrounding the crack tip being influenced by the tension surface of the specimen [1]. The finite element analyses indicated that the nonlinear stresses surrounding crack less than 15 mm (0.6 in.) deep were influenced by the tension surface. Thus indicating an increase in the toughness for flaw depths less than 15 mm (0.6 in.) would be expected.

Test Matrix

Two crack depths (one shallow and one deep) were tested during the development phase of the project. The nominal crack depth chosen was a ≈ 9 mm (a ≈ 0.4 in.), which is prototypic of the flaw depths that resulted in initiation in the IPTS studies [4-6]. One specimen was tested with a flaw depth of 14 mm (0.55 in.) for comparison. Presently, the relative influence of absolute crack depth, a, or normalized crack depth, a/W, is not fully understood. For the specimen sizes being considered in this project, it is believed that absolute crack depth rather than a/W will be the primary variable of interest. However, this assumption will be verified by testing additional crack depths during the production phase of the project.

To properly transfer shallow-crack fracture toughness data to the RPV, the effect of out-of-plane constraint on the toughness must be well understood. To investigate the effects of out-of-plane constraint in the beams, the beam thickness was varied to examine the effect on toughness. Three thicknesses were used: B= 50, 100, and 150 mm (2, 4, and 6 in.). At least one deep-crack specimen and two shallow-crack specimens were tested using beams of each thickness. The span for the 50 mm thick beam is 4W or 406 mm (16 in.). The spans for the 100 and 150 mm beams was increased to 864 mm (34 in.) in order to assure failure without exceeding the load capacity of the beam fixture.

The temperature for all developmental testing work is within the lower transition region for A533 B steel. RT_{NDT} for this material is -35 °C (-30 °F) [9]. The testing temperature for all the tests except one was T = -60 °C (-76 °F). T-RT_{NDT} was therefore -25 °C (-46 °F). One test was run at RT_{NDT}. During the production phase of the project testing will be performed at multiple temperatures in the lower transition region to fully quantify the temperature range in which the toughness elevation takes place.

Table 1 gives a summary of the development phase test matrix, showing the number of tests performed at each condition. A total of 14 specimens have been tested in this phase. Of the 14 beams tested, 5 were deep-cracked, and 9 were shallow (a/W = 0.10-0.15). Eight of the beams tested were 50 mm (2 in.) thick, 3 beams were 100 mm (4 in.)

thick, and 3 beams were 150 mm (6 in.) thick. All beams except one were tested at -60 °C (-76 °F). The final beam (B = 2 in., a/W = 0.1) was tested at -35 °C (-30 °F).

Test Technique

Instrumentation is attached to the specimens to make possible J-integral and CTOD measurement of fracture toughness. The J-integral is determined from the load-line-displacement (LLD) using the reference bar technique. CTOD is being determined from crack-mouth-opening-displacement (CMOD) using clip gages mounted on the crack mouth of the specimen. Currently, toughness data are being expressed in terms of CTOD according to ASTM E1290-89, Crack-Tip Opening Displacement (CTOD) Fracture Toughness Measurement.

The plastic component of CTOD is determined experimentally from the plastic component of CMOD and the rotation factor. The plastic displacement of the crack flanks is assumed to vary linearly with distance from the plastic center of rotation. In this way, the plastic CMOD can be related to the plastic CTOD. The plastic center of rotation is located ahead of the crack tip a distance equal to the rotation factor (RF) multiplied by the remaining ligament (W-a) [1]. Numerous experimental and analytical techniques have been used to determine the rotation factor [**1, 2, 11-15**], although no single technique seems to be universally accepted. The rotation factor in ASTM E1290 is given to be 0.4, but is a function of specimen geometry and material. In this study two experimental methods were used to determine the rotation factor. The first method was the use of dual clip gages located at different distances from the crack mouth. The second technique was to locate the neutral axis of the beam ahead of the crack tip using strain gages, assuming that the plastic center of rotation was located at the neutral axis of the beam. The strain gage method resulted in much more consistent and acceptable values of the rotation factor than the dual clip gage approach and was used for all CTOD calculations. The rotation factor was found to be insensitive to beam thickness and to vary between about 0.3 for the deep-crack specimens to 0.48 for the shallow crack specimens. The rotation factor for eight of the beams was determined using the strain gage method. The rotation factor for the other beams was taken as the average of the values based on crack depth. **Table 2** gives the rotation factor determined according to the preferred technique and the value used to determine the CTOD.

Two techniques were used to attach the clip gages to the specimens. The first technique was to attach the gage directly to the crack mouth; the second method was to attach the clip gage to a shim with a beveled edge which was welded to the specimen. Compliance values from each test were compared to expressions included in ASTM E813, J_{Ic}, A Measure of Fracture Toughness. Results of this comparison showed that attaching the clip gages to shims is the better technique. Data rrom the specimens in which the clip gages were attached directly to the crack mouth of the specimen were slightly in error. The error is due to lack of point contact between the clip gages and the specimen which introduces displacements other than opening of the crack-mouth in the clip gage measurement. Examination of the data shows, however, that correction of the error would have a negligible effect on the deep-crack data and would increase CTOD fracture toughness about 5-7% in the shallow-crack data. Since the exact correction is unknown for the beams in which the clip gages were attached directly to the specimen mouth and the errors are relatively minor, no adjustment of the data has been applied.

Initial notches were inserted into the specimens using electron discharge machining (EDM). The notches were then fatigue precracked to produce sharpened initial flaws. Fatigue precracking was performed according to the guidelines detailed in ASTM E399, Plane-Strain Fracture Toughness of Metallic Materials. Crack growth was monitored by

means of the change of crack mouth opening compliance, using the clip gage data and the equations for crack length in ASTM E813. The equations in ASTM E813 relating crack length to compliance are invalid for shallow-crack specimens. However, a change in compliance of 10-15% generally gave sufficient crack growth. In a few cases in the fatigue growth did not exceed 1.3 mm (0.050 in.). Examination of the results from these cases revealed no noticeable bias in the toughness values. After fracture, fatigue crack growth was visually measured according to the 9-point method as outlined in ASTM E813 or E1290. The greatest difference between any two crack growth measurements for all the tests was less than 1.8 mm (0.070 in.). The average maximum difference in crack growth measurements was about 0.9 mm (0.035 in.). Crack growth met all remaining requirements in ASTM E813 or E1290 for crack profile and orientation.

Test Results

Load versus CMOD curves were generated and examined for each beam tested. In order to normalize the load between beams of different spans, thicknesses and slightly different beam depths, the applied stress (rather than applied load) which would exist in an uncracked beam was plotted vs. CMOD. The applied stresses for the test and analyses results were calculated from the applied loads and the beam geometries according to elastic strength of materials equations. The stress vs. CMOD curves for the a/W = 0.50 and 0.10 tests are illustrated in **Fig. 1a and 1b**, respectively for beams tested at T = -60 °C (-76 °F) and are compared with the analytical stress vs. CMOD curve. The stress vs. CMOD test data are consistent and agree well with the analytical data providing additional confidence in the test data. The analytical stress vs. CMOD curves were generated using a plane strain elastic-plastic finite element ADINA [10] model. The test data represents beams of three different thicknesses. The consistency of the test data and the agreement with the plane-strain analytical data would indicate little loss of out-of-plane constraint due to insufficient specimen thickness in the test data.

The toughness data expressed in terms of CTOD and temperature in **Table 2** are shown in **Fig. 2** along with the material characterization curve [9]. Data from three crack depths (a/W = 0.50, 0.15, and 0.10) and three thicknesses (B = 50, 100, 150 mm) are presented. The deep-crack toughness values are slightly higher than the material characterization curve and are consistent with previous compact-tension specimen data [16] from the same heat of material tested prior to this program. The trend of the results in **Fig. 2** indicates both a significant increase in the measured fracture toughness for shallow-crack specimens in the lower transition region. The a/W = 0.15 datum also appears to exhibit a shallow-crack toughness elevation. The ratio of the mean shallow-crack toughness to deep-crack toughness is 4.4 for the beams tested at -60 C (-76 F). The ratio of the shallow to deep lower-bound toughness is 2.9 which is consistent with the shallow-crack elevated toughness for A36 and A517 steel determined at the University of Kansas [1, 2]. As indicated in **Ref. 1 & 2**, the shallow and deep-crack toughness for A533 B is expected to converge on the lower shelf.

Crack-tip-opening displacement CTOD and the plane-strain stress-intensity factor, K_{Ic} are related according [17] to:

$$CTOD = K_{Ic}^2(1-\nu^2) / (2\sigma_y E). \qquad (1)$$

The ratio of shallow-to-deep toughness in terms of K_{Ic} is equal to the square root of the ratio in terms of CTOD (shallow-crack toughness is ≈70% greater than the deep-crack toughness at -60 ° C). The spread of the data is also reduced expressing the toughness in terms of K_{Ic}.

If it is assumed that the shallow-crack toughness curve has the same shape as the deep-crack toughness curve, the shallow-crack toughness increase can be expressed as a

temperature shift. Previous A36 data supports this assumption [1]. The lower bound shallow-crack datum at T = -60 °C (-76 °F) and the single datum at T = -35 °C (-30 °F) are shifted 46 to 48 °C (83 to 87 °F) from the characterization curve respectively. The lower bound deep-crack datum is shifted about 16 °C (28 °F) from the characterization which indicates a temperature shift for the shallow-crack specimens of 30 °C (55 °F).

Beams 50, 100, and 150 mm (2, 4, and 6 in.) thick were tested to investigate the influence of differing out-of-plane-constraint levels on the toughness of shallow and deep-crack specimens. Toughness data are plotted as a function of beam thickness for all of the tests conducted at T = -60 °C (-76 °F) in **Fig. 3.** As shown in **Figs. 2 and 3,** the toughness values for the shallow and deep-crack specimens from the 100 and 150 mm (4 and 6 in.) thick beams are generally consistent with the 50 mm (2 in.) thick data. However, there appears to be slightly more data scatter associated with the 50 mm (2 in.) thick beams than with the 100 and 150 mm (4 and 6 in.) thick beams. It is interesting to note that the lowest shallow and deep-crack toughness values were both from beams with the least thickness (B = 50 mm). Beams of three thicknesses were tested to select the appropriate beam size for the production phase testing. The testing temperature is expected to be greater for many of the beams tested in the production phase of the program. As the temperature increases, additional loss of out-of-plane constraint is anticipated. Therefore, even though the 50 mm beam thickness might be sufficient at lower temperatures, the 100 mm beam thickness was chosen for future testing since the greater thickness might be required at the higher temperatures.

Modified Irwin Correction

The toughness data were converted to K_C, critical stress-intensity factor values according to the following equation [18]:

$$K_C = \{m\sigma_y E^* CTOD\}^{1/2}. \quad (2)$$

It was decided to set the constraint factor, m, to 2 for deep and shallow-flaw specimens until additional information was available on the variation of the constraint parameter for shallow flaws. Examination of the K_C data and ASTM E399 revealed that only the 150 mm (6 in.), deep-crack test result would meet the validity requirement for sufficient beam thickness and none of the data would meet the validity requirement for crack depth. The plane stress form of Eqn. 2 was used since the data did not satisfy the ASTM E399 validity requirements. The goal of the shallow crack program is to investigate the toughness as a function of crack depth and apply the results to a reactor pressure vessel, which is a highly constrained application. The deep crack test results therefore should maintain plane-strain constraint or be adjusted to estimate the plane-strain toughness. Since specimens required to maintain plane-strain constraint are prohibitively large, the data taken from the deep-crack specimens have been adjusted for loss of out-of-plane constraint via Irwin's β_C correction [19]. The Irwin β_C correction is first applied by calculating β_C from the experimental data and then solving the following equation for β_{IC}:

$$1.4\beta_{IC}^3 + \beta_{IC} = \beta_C \text{, where:} \quad (3a)$$

$$\beta_C = (K_C/\sigma_y)^2 / B, \text{ and} \quad (3b)$$

$$\beta_{IC} = (K_{IC}/\sigma_y)^2 / B. \quad (3c)$$

The adjusted, plane-strain toughness is then calculated according to :

$$K_{IC} = K_C \sqrt{(\beta_{IC}/\beta_C)}. \quad (4)$$

Application of the Irwin β_C correction reduces the average deep-crack critical toughness from 109 MPa$\sqrt{m}$ (99.2 Ksi$\sqrt{in.}$) to a corrected plane-strain value of 90.5 MPa$\sqrt{m}$ (82.4 Ksi$\sqrt{in.}$) as shown in **Table 3.** The magnitude of the reduction is relatively minor [19].

The small magnitude of the correction and the consistency between the data of different thicknesses indicate that little loss of out-of-plane constraint is present in the deep-crack data in spite of the fact that the validity requirements have not been met.

Relaxation of crack-tip constraint in either direction (in-plane or out-of-plane), has the effect of elevating the critical toughness. The Irwin β_c correction successfully accounts for loss of out-of-plane constraint and, therefore, a modification (of the β_c correction) proposed by Merkle [20] to account for the loss of in-plane constraint associated with shallow flaws was applied. This modification is based on the assumption that the critical dimension in the constraint of a beam is the distance from the point of greatest constraint to the nearest free surface, not including the crack surface. In deep-crack beams, this distance is half the beam thickness; in shallow-crack specimens, the critical dimension is the crack depth. By using the appropriate critical dimension, the Irwin β_c correction can be modified to account for both loss of out-of-plane constraint (insufficient thickness) and loss of in-plane constraint (shallow-crack effect) [20]. As shown in **Table 3** and **Fig. 4**, the modified Irwin correction applied to the HSST data adjusts both deep and shallow-crack toughness data to the same value.

Since the shallow and deep-crack toughness data can be adjusted to the same value, the modified correction could potentially be used to "predict" the shallow-crack fracture toughness from deep-crack toughness data. Although the shallow-crack toughness data were available, the modified Irwin correction was applied to the data to see if "predictions" could be made of the shallow-crack toughness using only deep-crack data. The "predicted" shallow-crack toughness was determined from the adjusted plane-strain, deep-crack toughness according to [20]:

$$K_c = K_{Ic} * [1 + 1.4\beta_{Ic}^2]^{1/2}, \quad (5)$$

where K_{Ic} = 90.5 MPa$\sqrt{m}$ (82.4 Ksi$\sqrt{in.}$) and

$$\beta_{Ic} = (K_{Ic} / \sigma_y)^2 / 2a . \quad (6)$$

The agreement between the "predicted" shallow-crack toughness estimated using the modified Irwin correction and the actual toughness from the shallow-crack specimens is good. The average "predicted" shallow-crack toughness using the deep-crack data with the modified Irwin β_c correction is 230 MPa$\sqrt{m}$ (209 Ksi$\sqrt{in.}$); the average actual shallow-crack toughness is 229 MPa$\sqrt{m}$ (208 Ksi$\sqrt{in.}$). A plot of the actual vs. "predicted" toughness for each shallow-crack test (**Fig. 5**) shows good agreement between the individual "predicted" and actual shallow-crack toughness values. It should be noted that the modified Irwin correction "predicted" the shallow-crack toughness for crack depths ranging between a = 8.36 to 14.0 mm (0.329 to 0.553 in.). The "predicted" shallow-crack toughness shows little scatter since the individual values only vary with the crack depth. The ability of the modified Irwin β_c correction to predict the elevated shallow-crack toughness from deep-crack data depends on similar out-of-plane constraint being present in the data of different thicknesses.

Future Work

The application of the shallow-crack fracture toughness data to reactor vessel analyses remains the final goal of the program. To reach that goal, more specimens should be tested with multiple crack depths and at several temperatures within the transition region. The results generated to date are encouraging but not conclusive as to how to apply the data to an RPV. Prior experimental work within the HSST program has included tests on thick-walled vessels which have contained relatively shallow flaws [21]. These tests offer a means to validate the technology of applying shallow-flaw toughness data to an RPV.

In addition, numerical analyses of the test specimen and the application (i.e. an axially oriented flaw in an RPV) need to be performed and interpreted. These analyses will provide a means for checking transferability of the test results to an RPV. The modified Irwin correction is being further evaluated and refined and is being considered as a relationship to account for flaw-depth in the fracture toughness of reactor pressure vessel steels. The conditions under which the modified Irwin correction can be used in reactor vessel analyses need to be established.

Conclusions

Although the test results presented in this paper are preliminary, the data are encouraging and the following interim conclusions can be drawn.

Specimens tested with a shallow-crack depth ($a \approx 9$ mm, in this case), exhibit a toughness which is significantly higher than the deep-notch toughness at temperatures in the lower transition region. The shallow-crack fracture toughness data determined for A533 B are consistent with the toughness elevation observed by others for shallow-cracks in A36 and A517 steels.

The single specimen tested with a crack depth of 14 mm (0.6 in.) also appears to show a toughness elevation.

The shallow-crack toughness elevation from the 100 and 150 mm (4 and 6 in.) thick beams is generally consistent with the 50 mm (2 in.) thick data. However, there appears to be slightly more data scatter associated with the 50 mm thick beams than with the 100 and 150 mm thick beams. The influence of out-of-plane constraint appears minimal in the test results.

The Irwin β_C correction, modified to account for loss of in-plane constraint, has been used to estimate the elevated shallow-crack fracture toughness from the deep-crack toughness data. The agreement between the estimated shallow-crack toughness estimated using the modified Irwin correction and the actual toughness from the shallow-crack specimens is good.

Acknowledgements

This work is being sponsored through the Office of Nuclear Regulatory Research, U.S. Nuclear Regulatory Commission, monitored by M. E. Mayfield. The technical assistance of the HSST staff and subcontractors is gratefully acknowledged.

References

1. W. A. Sorem, R. H. Dodds, Jr., and S. T. Rolfe, "An Analytical Comparison of Short Crack and Deep Crack CTOD Fracture Specimens of an A36 Steel, *WRC Bulletin 351*, Welding Research Council, New York, NY 10017, February 1990.

2. J. A. Smith, and S. T. Rolfe, "The Effect of Crack Depth to Width Ratio on the Elastic-Plastic Fracture Toughness of a High-Strength Low-Strain Hardening Steel," *WRC Bulletin 358*, Welding Research Council, New York, NY 10017, November 1990.

3. T. J. Theiss, "Recommendations for the Shallow-Crack Fracture Toughness Testing Task Within the HSST Program," USNRC Report NUREG/CR-5554 (ORNL/TM-11509), August 1990.

4. R. D. Cheverton and D. G. Ball, "Pressurized-Thermal-Shock Evaluation of the H. B. Robinson Nuclear Power Plant," USNRC Report NUREG/CR-4183 (ORNL/TM-9567/V1), September 1985, pp. 263-306.

5. R. D. Cheverton and D. G. Ball, "Pressurized-Thermal-Shock Evaluation of the Calvert Cliffs Nuclear Power Plant," USNRC Report NUREG/CR-4022 (ORNL/TM-9408), September 1985, pp. 201-44.

6. R. D. Cheverton and D. G. Ball, "Preliminary Development of an Integrated Approach to the Evaluation of Pressurized Thermal Shock as Applied to the Oconee 1 Nuclear Power Plant," USNRC Report NUREG/CR-3770 (ORNL/TM-9176), May 1986, pp. 5.1-5.51.

7. T. L. Dickson and T. J. Theiss, "Potential Impact of Enhanced Fracture-Toughness Data on Pressurized-Thermal-Analysis," Proceedings of the U.S Nuclear Regulatory Commission Eighteenth Water Reactor Safety Meeting, Rockville, Md., October 22-24, 1990, USNRC Report NUREG/CP-00, March 1991.

8. T. J. Theiss, G. C. Robinson, and S. T. Rolfe, "Preliminary Test Results from the Heavy-Section Steel Technology Shallow-Crack Toughness Program", Proceedings of the ASME Pressure Vessel & Piping Conference; Pressure Vessel Integrity Session, San Diego, CA., June 23-27, 1991, (in preparation).

9. D. J. Naus, "SEN Wide-Plate Crack-Arrest Tests Using A533 Grade B Class 1 Material: WP-CE Series," USNRC Report NUREG/CR-5408 (ORNL/TM-11269), November 1989.

10. K. J. Bathe, "ADINA-87, A Finite Element Program for Automatic Dynamic Incremental Nonlinear Analysis," MIT Report 82448-1, 1975.

11. Cottrell, B., Li, Q.-F., Zhang, D.-Z. and Mai, Y.-W., "On the Effect of Plastic Constraint on the Ductile Tearing in a Structural Steel," *Eng. Frac. Mech.*, **21** (2), 239-244 (1985).

12. Li, Q.-F., "A Study About J_i and δ_i in Three-Point Bend Specimens With Deep and Shallow Notches," *Eng. Frac. Mech.*, **22** (1), 9-15 (1985).

13. Zhang, D.-Z. and Wang, H., "On the Effect of the Ratio a/W on the Value of δ_i and J_i in a Structural Steel," *Eng. Frac. Mech.*, **26** (2), 247-250 (1987).

14. Matsoukas, G., Cottrell, B. and Mai, Y.-W.., "On the Plastic Rotation Constant Used in Standard COD Tests," *Int. J. Fract.*, **26** (2), R49-R53 (1984).

15. Anderson, T. L., McHenry, H. I., and Dawes, M. G., **"Elastic-Plastic Fracture Toughness Tests with Single-Edge Notched Bend Specimens,"** *Elastic-Plastic Fracture Test Methods: The User's Experience, ASTM STP 856*, E. T. Wessel and F. J. Loss, Eds., American Society for Testing and Materials, 1985, pp. 210-229.

16. D. J. Ayres et. al., *Tests and Analyses of Crack Arrest in Reactor Vessel Materials*, Appendix G, "Material Characterization," EPRI NP-5121SP, April 1987.

17. Barsom, J. M. and Rolfe, S. T., *Fracture and Fatigue Control in Structures*, Prentice-Hall, Englewood Cliffs, NJ, 1987.

18. Dawes, M. G., **"Elastic-Plastic Fracture Toughness Based on the COD and J-Contour Integral Concepts,"** *Elastic-Plastic Fracture, ASTM 668*, J. D. Landes, J. A. Begley, and G. A. Clarke, Eds., American Society for Testing and Materials, 1979, pp. 307-333.

19. J. G. Merkle, "An Examination of the Size Effects and Data Scatter Observed in Small-Specimen Cleavage Fracture Toughness Testing," USNRC Report NUREG/CR-3672 (ORNL/TM-9088), April 1984.

20. Merkle, J. G., **"An Approximate Method of Elastic-Plastic Fracture Analysis for Nozzle Corner Cracks,"** *Elastic-Plastic Fracture, ASTM 668*, J. D. Landes, J. A. Begley, and G. A. Clarke, Eds., American Society for Testing and Materials, 1979, pp. 674-702.

21. Cheverton, R. D., Iskander, S. K., and Ball, D. G., **"Review of Pressurized-Water-Reactor-Related Thermal Shock Studies,"** *Fracture Mechanics: Nineteenth Symposium, ASTM STP 969*, T. A. Cruse, Ed., American Society for Testing and Materials, Philadelphia, 1988, pp. 752-766.

List of Tables

1. Test Matrix for HSST Development Beams
2. HSST Development Beam Data
3. Actual and Predicted Toughness Values Using Modified Irwin β_c Correction

List of Figures

1a. Applied Stress vs. CMOD for a/W = 0.50 Beams
1b. Applied Stress vs. CMOD for a/W = 0.10 Beams
2. HSST Test Data With Material Characterization Curve and Previous Compact Tension Data
3. HSST Test Data at Three Thicknesses Tested at -60 °C
4. Application to Modified Irwin β_c Correction to Deep and Shallow-Crack Toughness Data
5. Agreement Between Actual and "Predicted" Toughness Using Modified Irwin β_c Correction for Shallow-Crack Specimens

Table 1. Test Matix for HSST Developement Beams

Thicknesses	Crack Depths, a/W			
	0.50	0.15	0.10	Total
50 mm	3 beams	1 beam	4 beams	8 beams
100 mm	1 beam		2 beams	3 beams
150 mm	1 beam		2 beams	3 beams
Total	5 beams	1 beam	8 beams	14 beams

Notes:

1 All beams were tested at T ≈ –60 °C (–76 °F) except one of the 50 mm, a/W = 0.10 beams which was tested at T ≈ –35 °C (–30 °F).

2. Nominal beam depth was 94 mm (3.7 in.).

Table 2. HSST Test Data

HSST Beam #	Temperature (°C)	S (mm)	B (mm)	W (mm)	a (mm)	a/W	Rotation Factor	Measured Elastic Compliance (mm/kN)	Failure Load (kN)	Measured Failure CMOD (mm)	Toughness CTOD (mm)
3	−35.6	406	50.6	99.7	10.0	0.102	0.47	3.09×10^{-4}	600	0.808	0.587
4	−60.6	406	50.7	99.5	51.8	0.520	0.30[1]	3.38×10^{-3}	128	0.461	0.0469
5	−55.3	406	50.6	99.1	51.2	0.517	0.30[1]	3.14×10^{-3}	140	0.442	0.0488
6	−59.2	406	50.6	99.5	51.9	0.522	0.30[1]	3.52×10^{-3}	185	0.758	0.109
7	−59.4	406	50.7	94.2	10.2	0.108	0.47[1]	3.27×10^{-4}	483	0.250	0.138
8	−59.5	406	50.8	94.2	9.63	0.102	0.50	3.12×10^{-4}	657	0.652	0.478
9	−62.3	406	50.9	94.0	9.52	0.101	0.47	3.09×10^{-4}	552	0.508	0.352
10	−60.2	406	50.9	94.3	14.0	0.149	0.45[1]	4.77×10^{-4}	489	0.434	0.232
11	−56.7	864	102	93.9	8.36	0.0890	0.48	3.08×10^{-4}	472	0.312	0.198
12	−56.7	864	102	94.7	49.8	0.526	0.26	4.44×10^{-3}	117	0.574	0.0560
13	−59.6	864	102	94.0	8.81	0.0938	0.48[1]	3.29×10^{-4}	502	0.514	0.360
14	−57.4	864	152	92.5	8.69	0.0939	0.48	2.25×10^{-4}	723	0.504	0.349
15	−58.5	864	153	94.5	8.66	0.0917	0.47	2.14×10^{-4}	684	0.257	0.147
16	−57.8	864	153	94.0	50.0	0.532	0.33	2.81×10^{-3}	170	0.530	0.0576

Notes:

1. Rotation factor not explicitly determined for these specimens. Rotation factor used is average of similar tests.

2. Yield Stress = 468 MPa @ T ≈ -60 °C and 440 MPa @ T ≈ -35 °C. The Yield Stress was estimated from room temperature values and adjusted for the lower temperatures.

Table 3. Actual and "predicted" toughness values using modified Irwin βc correction

HSST Beam #	a (mm)	B (mm)	K_c actual $(MPa\sqrt{m})$	K_{Ic} $(MPa\sqrt{m})$	K_c predicted $(MPa\sqrt{m})$
4	51.8	50.7	95.2	79.1	109
5	51.2	50.6	97.3	80.1	110
6	51.9	50.6	145	99.7	132
12	49.8	102	104	94.2	100
16	50.0	153	105	99.6	95.9
Average Deep-Flaw			109	90.5	109
7	10.2	50.7	163	81.0	216
8	9.63	50.8	304	101	227
9	9.52	50.9	261	95.0	229
10	14.0	50.9	212	99.0	169
11	8.36	102	196	81.9	256
13	8.81	102	264	93.0	245
14	8.69	152	260	92.0	247
15	8.66	153	168	78.1	248
Average Shallow-Flaw			229	90.1	230

Note:

1. Average of deep-crack adjusted values was used to "predict" toughness for shallow-flaw specimens.
2. Only tests conducted at T = –60°C included.

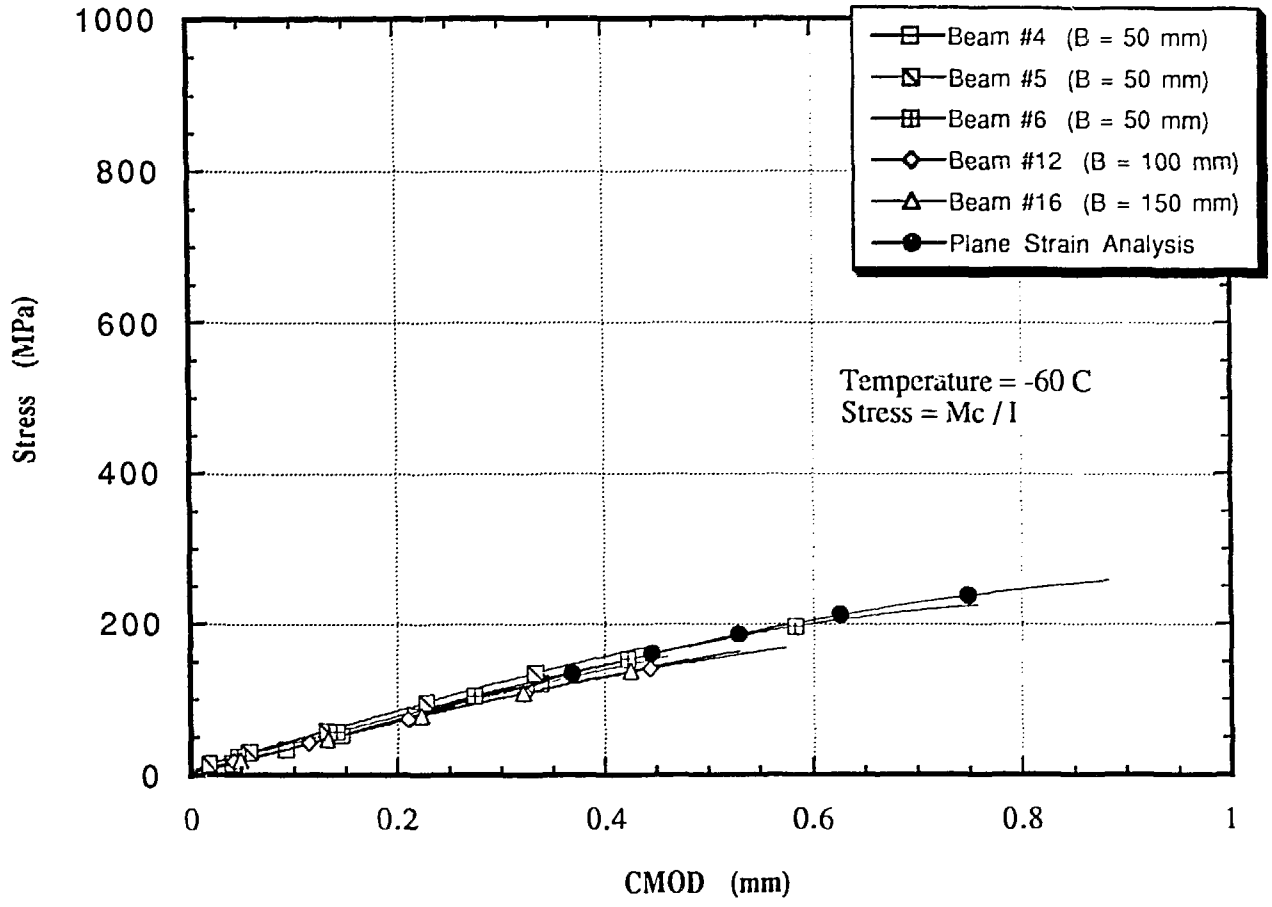

Fig. 1a Applied Stress vs. CMOD for a/W = 0.50 Beams

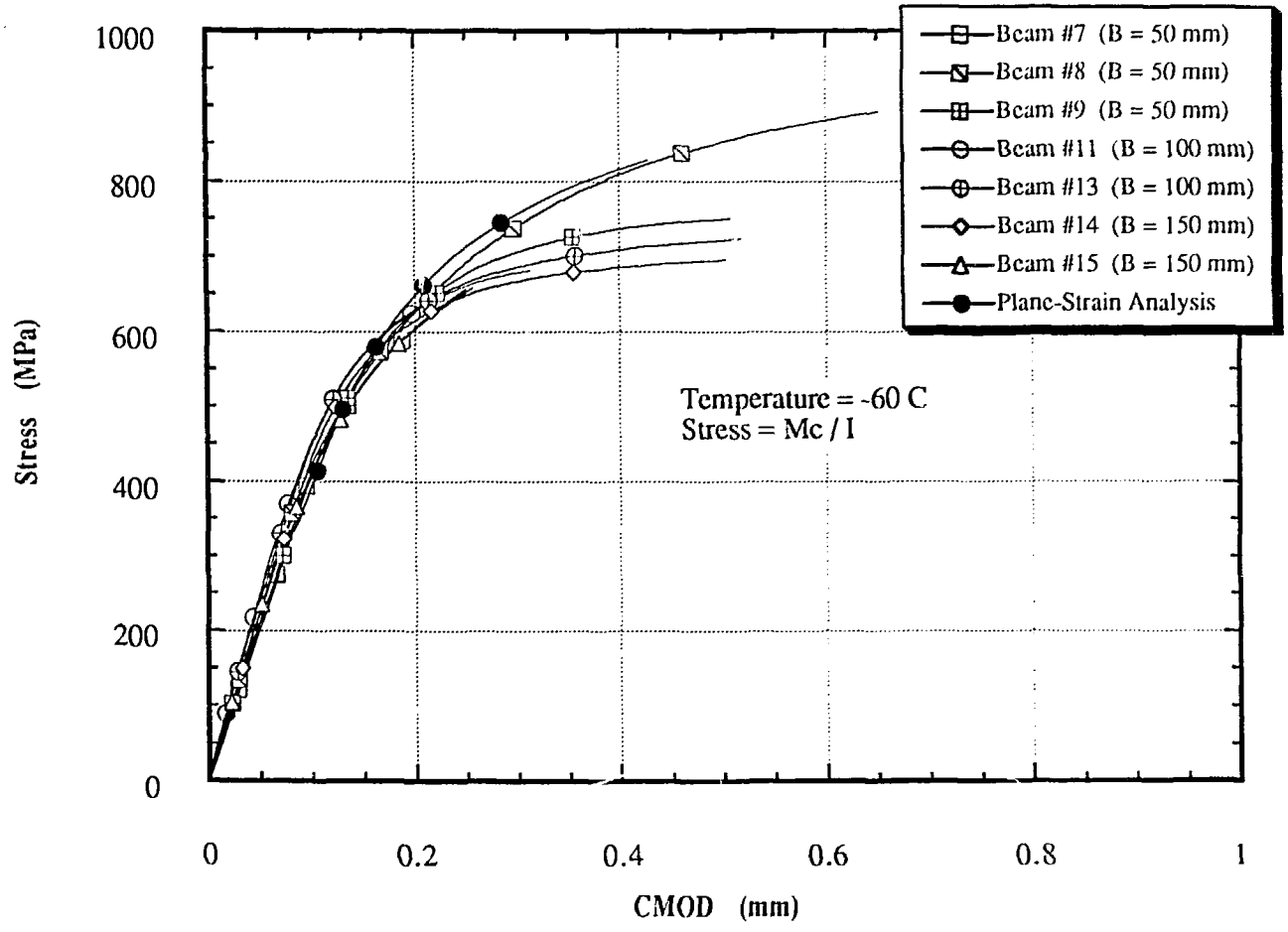

Fg. 1b Applied Stress vs. CMOD for a/W = 0.10 Beams

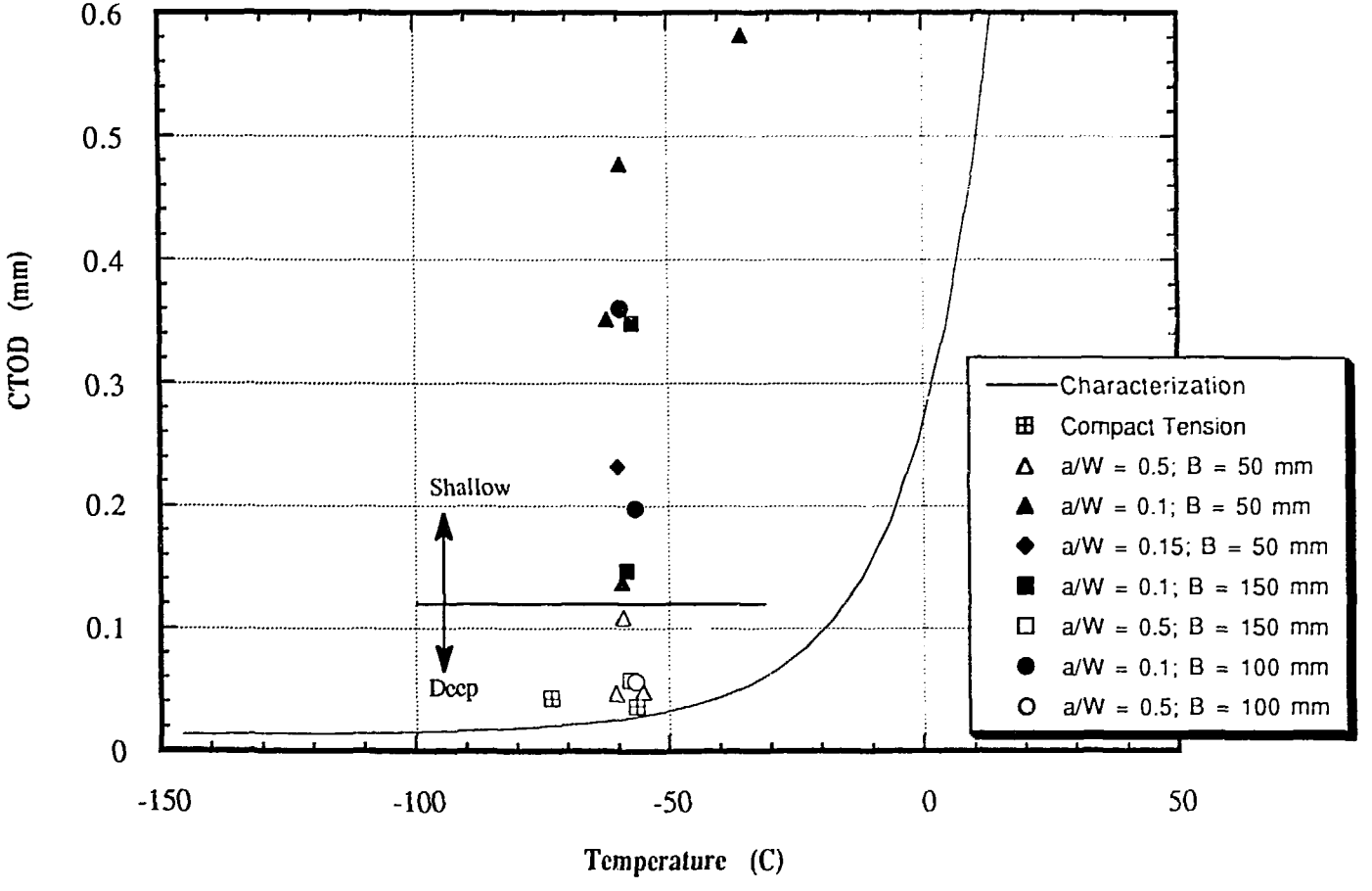

Fig. 2 HSST Test Data With Material Characterization Curve and Previous Compact Tension Data.

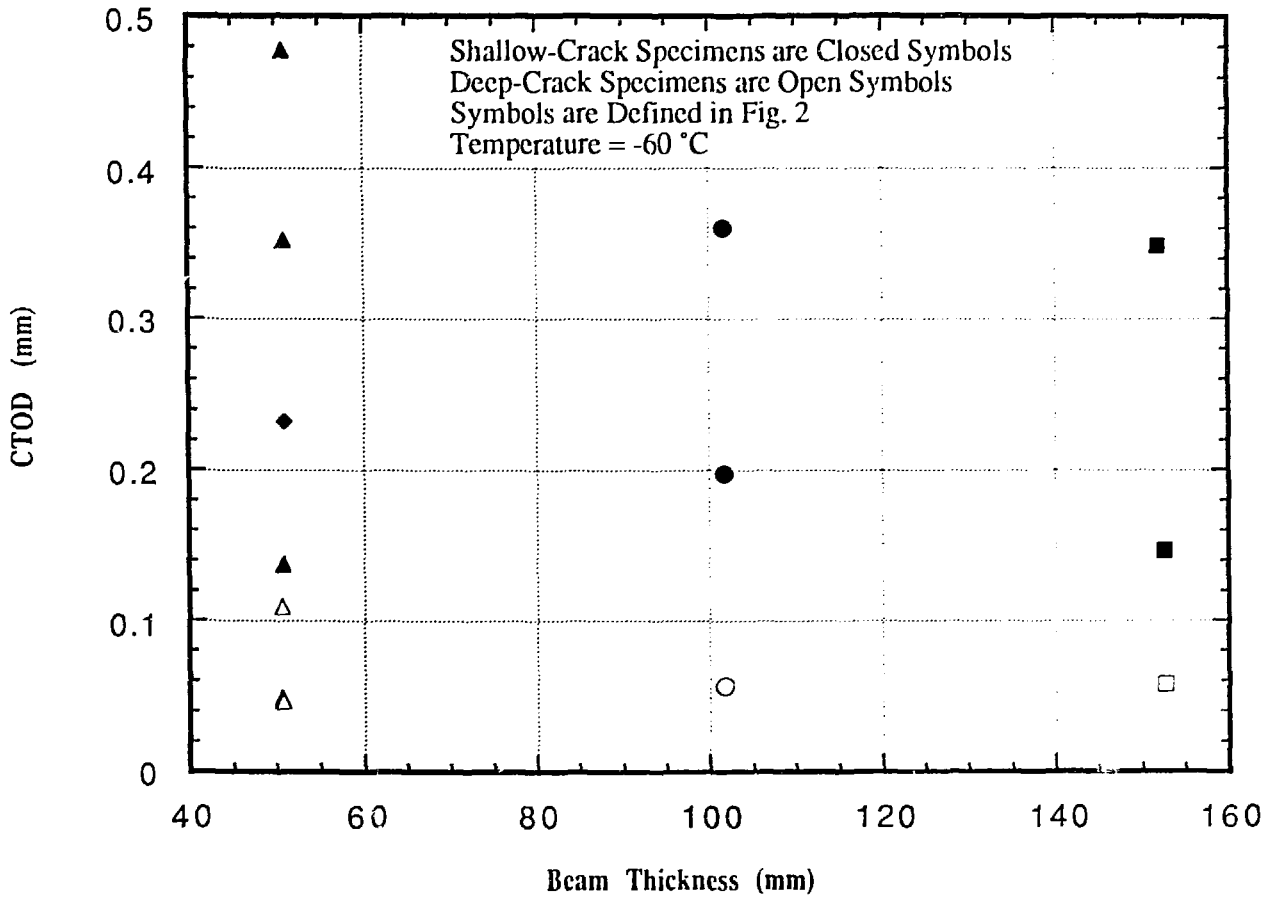

Fig. 3 HSST Test Data At the Three Thickness Tested at - 60 °C

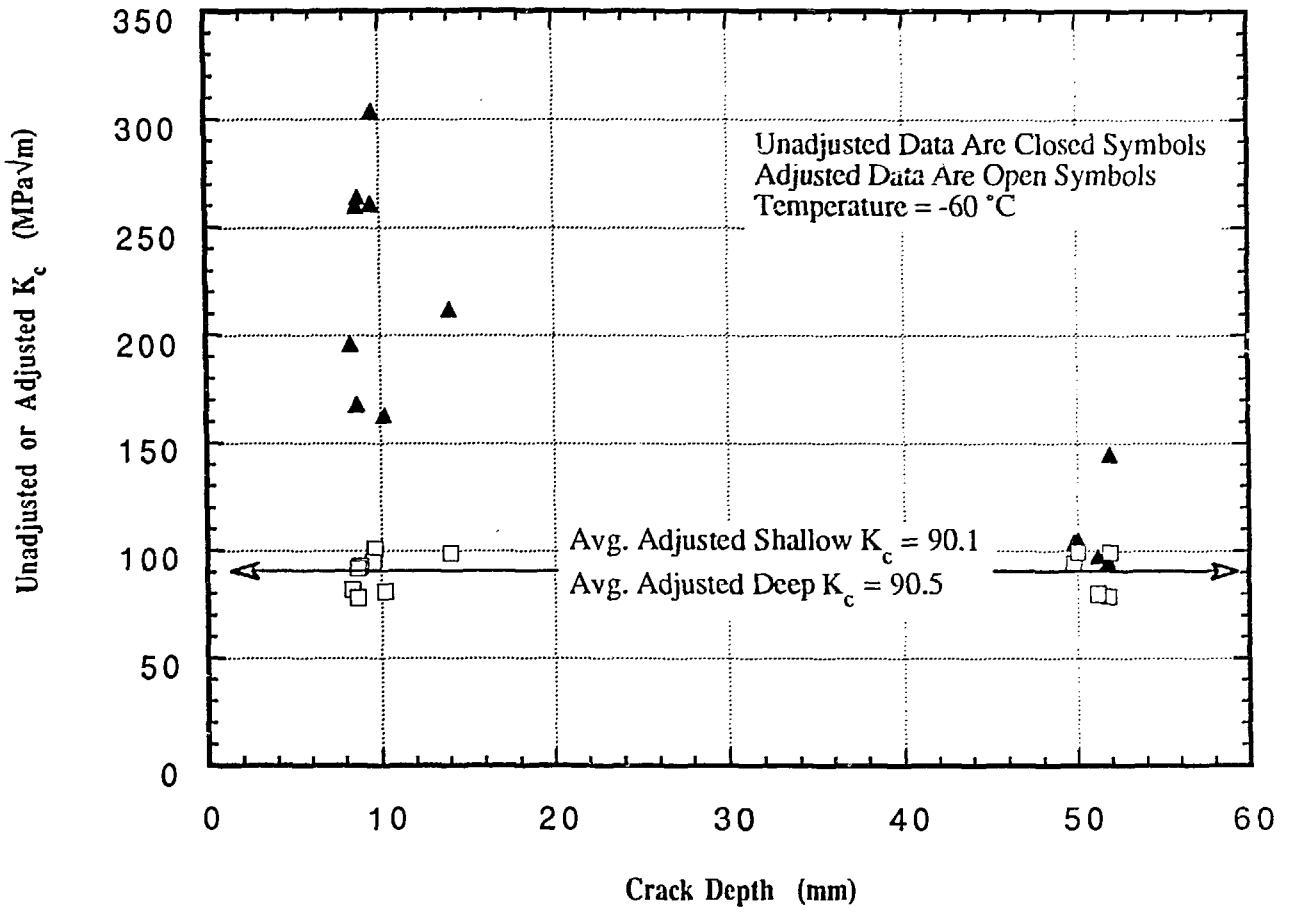

Fig. 4 Application of Modified Irwin $ß_c$ Correction to Shallow and Deep-Crack Toughness Data

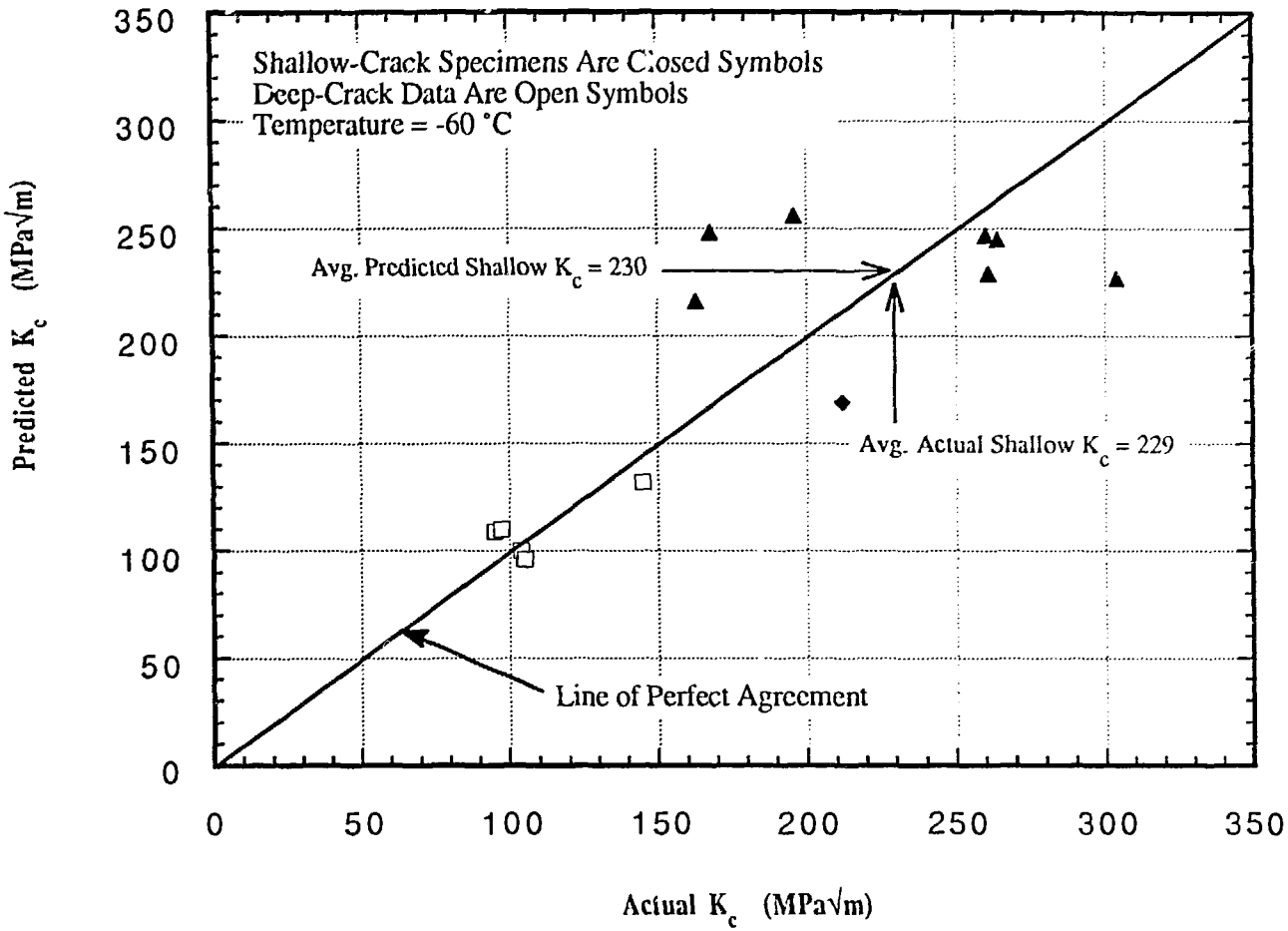

Fig. 5 Agreement Between Actual and "Predicted" Toughness Using the Modified Irwin $ß_c$ Correction for Shallow-Crack Specimens